

Spatial fluctuations and anomalous reaction order in a reactive scheme involving a cooperative full desorption

P. Córdoba-Torres,¹ R. P. Nogueira,² and V. Fairén^{1,*}

¹*Departamento de Física Matemática y Fluidos, UNED, Apdo. 60141, 28080 Madrid, Spain*

²*UPR 15 of CNRS, "Laboratoire Interfaces et Systèmes Electrochimiques," Université Pierre et Marie Curie, C.P. 133, 4 Place Jussieu, 75252 Paris Cedex 05, France*

(Received 23 February 2004; revised manuscript received 30 June 2004; published 29 December 2004)

Anomalous reaction rates have been found in the hydrogen desorption of H-terminated surfaces in semiconductor epitaxy, with a reaction order shifting from two to one, or even taking fractional values. We analyze the issue in terms of a cooperative full desorption (CFD) reaction $A+A \xrightarrow{k_3} S+S$, coupled to an adsorption reaction $S \xrightarrow{k_1} A$ and an alternative desorption route $A \xrightarrow{k_2} S$. Steady state properties of the three-step reactive scheme are analyzed in a one-dimensional lattice in the absence of diffusion. Microscopic Monte Carlo simulations show anomalous spatial distributions of reactants in the stationary state: depending on the reaction rate constants of the overall scheme, either a local "aggregation" or a local "dispersion" of A -particles is observed. The CFD reaction itself is well described by a fractional order kinetics that takes into account these anomalies and that depends on the kinetic rate constants of the overall adsorption-desorption reaction mechanism. The problem is addressed with an analytical approach for the *active neighborhood* of a reactant, which provides a closed expression of the reaction order as a function of the kinetic parameters. This approach is in excellent agreement with numerical simulations. Spatial correlations, as well as fluctuation correlations, are also formalized in terms of the kinetic constants. We discuss the results in the context of the hydrogen evolution reaction on silicon surfaces.

DOI: 10.1103/PhysRevE.70.061108

PACS number(s): 05.40.-a, 82.20.Wt, 82.40.Np

I. INTRODUCTION

Identification of mechanisms for surface reactions and knowledge of their corresponding rates has become a topic of considerable interest because of its technological implications. One of such reactions, to which much attention has been devoted in the literature, is the one-species annihilation reaction $A+A \rightarrow 0$, also known as cooperative full desorption (CFD) when it happens between adsorbed particles. This reaction is of particular importance within the context of hydrogen chemistry on semiconductor surfaces [1] because of its key role in pregrowth, growth, and postgrowth treatment, though fundamental aspects of H-terminated surfaces are far from being understood [2–4] despite two decades of extensive experimental and theoretical work. In gas source chemical vapor deposition (GS-CVD) epitaxy, for example, the use of silane (SiH_4) or disilane (Si_2H_6) as precursors has proved to yield a very selective low-temperature epitaxy [5–8]. Upon adsorption, a Si_2H_6 molecule undergoes a series of reactions leading to a surface coverage by a mixture of Si-hydrides, the composition of which is dependent on experimental conditions [6,7]. Hydrogen finally desorbs via different surface reactions. For example, in ultrahigh vacuum CVD for the case of Si(100), molecular hydrogen forms by recombination at localized monohydride dimers (H-Si-Si-H) [6,9,10]. Wetterauer *et al.* [11] found that this pathway is supplemented by single atom photodesorption from a hydro-

genated Si(111) surface. In plasma-enhanced CVD growth of hydrogenated amorphous and microcrystalline silicon, which are emergent alternatives to crystalline Si in many electronic devices, impinging hydrogen gas atoms recombine with Si-hydrides but also with bonded hydrogen surface atoms to form H_2 .

For obvious reasons, knowledge of the reaction rate of the hydrogen CFD is crucial [2]. In some instances it does not necessarily obey the second-order kinetics that one would expect from the traditional model of encounters between hopping hydrogen atoms. Early experimental studies [12] already concluded on a first order reaction for molecular hydrogen desorption from the monohydride phase on Si(100), though more recent work by Nakazawa and coworkers [9,10] points at fractional reaction orders between 1 and 2 depending on the hydrogenating gas and thermal history. A shift from second order at low H coverage to first order at high H coverage has also been reported [4]. Several explanations have been provided for this unsuspected behavior. Substrate dimers have two unsaturated dangling bonds that can be terminated by hydrogen. An early model [12] invoked the interaction of an excited H atom with a localized, chemisorbed hydrogen. The overall process is limited by the excitation reaction and consequently the desorption is first order. Later, the idea of "preparing" of H atoms to form a doubly occupied dimer [13] gained momentum and most models conform now to it. There is a suspicion for adsorption-desorption occurring from a combination of two different pathways involving intra- (H_4) and interdimer (H_2) configurations [2,4], with a reaction order dependent on which configuration dominates, although much work remains to be

*Corresponding author. FAX: (+34) 913987628. Email address: vfairen@dfmf.uned.es

done to unravel the actual mechanism. Nakazawa *et al.* [10] examined separately prepairing and desorption. Starting from standard, mean field rate equations the authors argued that the coverage fraction of isolated hydrogen atoms is a representation of the fractional reaction order. However, this fractional reaction order is not explicitly taken into account in their formulation. An intermediate reaction order has been also found for the Si(111) surface following chemisorption of disilane [14].

We shall presently invoke the simplest scenario, which involves the prepairing of two single occupied monohydride dimers (H-Si-Si-) forming a doubly occupied monohydride dimer (H-Si-Si-H), the hydrogens of which recombine liberating H₂. The hydrogen evolution on the surface can thus be represented in terms of a very simple, lumped model mechanism involving single occupied monohydride dimers (SOD) as fundamental units:



where S and A mean a clean substrate dimer and an SOD, respectively. Decomposition of high order hydrides yields H atoms that can attach themselves to clean substrate dimers yielding SOD—reaction (1). Also, hydrogen from a SOD can hop to an neighboring unsaturated dangling bond leaving a substrate dimer [6]—reaction (2). Finally, interdimer transfer of a hydrogen atom between two adjacent SOD give a doubly occupied monohydride dimer (DOD) and a clean substrate dimer—reaction (3). Molecular hydrogen desorbs from the DOD—reaction (4). Desorbing molecules have low translational energy, showing no sign of having traversed an energy barrier. We can thus assume hydrogen desorption from a DOD to be very fast such that $k'_4 \gg k'_3$, i.e., the prepairing reaction (3) is rate limiting. As a matter of fact, Step (4) will be disregarded in simulations and a successful prepairing will be considered as liberating two contiguous substrate dimers. Reaction (3) takes then the CFD definitive form:



Inconsistencies in the kinetics behavior of the CFD reaction with respect to the classical chemical rate equations—based on the mean field approach (MFA)—are well known when the dimensionality of the support in which the reaction takes place is below some critical dimension. This “anomalous” kinetics has been found to be closely connected to many-particle effects [15,16]. Spatial fluctuations of particle density in certain volumes lead to correlated spatial distribu-

tion of reactants and a tendency to local ordering of the surviving particles [17,18]. This chemical self-organization arises as a consequence of the interplay between the CFD mechanism itself, which introduces ordering in the system by generating depletion zones around particles that slow down the reaction with respect to the MFA, and homogenizing mechanisms such as diffusion or random input of particles. The ability of the system to offset correlations introduced by the reaction determines the kinetics of the process.

Most of the work on anomalous kinetics has been devoted to study the influence on the development of fluctuations of such items as the topological characteristics of the substrate where the reaction takes place, the diffusion properties of the reactants, the mechanism of reaction, or the input of particles. When the process is diffusion-controlled, both in transient [19–25] and steady-state [26–28] reactions, self-ordering is observed in low dimensions ($d < 2$) because the mixing effect of diffusion is not as effective as it is in higher dimensions. Correlation length scales and characteristic time scales depend on the external source rate and on the diffusivity. The CFD reaction rate is described in both cases with the same reaction order [29], which in turn depends on the dimensionality of the support, on the characteristics of diffusion [30], and on the mode of reactant input [28]. It does not depend, however, on the input rate and on the reaction probability. For one-dimensional systems, when Brownian diffusion and random input of particles are considered, the reaction order is found to be 3 [28,29,31], different from the classical MFA value of 2.

The role of fluctuations for immobile reactants is even more essential because the smoothing influence of diffusion is absent. The situation in which long-range reactions are allowed has attracted particular interest [32–34]. In the transient regime case, correlations between surviving particles increase as reaction proceeds, showing a spatial self-ordering (depletion zone) qualitatively similar to that obtained in diffusion limited circumstances [34]. The asymptotic behavior of fluctuations and reactant self-ordering depend on the spatial dimensionality and on the transfer rate type, leading again to a nonclassical decay of the density of particles. The effect of local fluctuations is naturally enhanced for short-range interactions, especially when reactions occur between nearest neighbors in low dimensions [35–39]. The results exhibit an explicitly nonuniversal, initial condition dependent behavior, persistent at all times and, again, not consistent with the mean-field rate. Steady-state behavior has also been examined, showing also an anomalous dependence of the steady-state particle density on the input rate both for long-range [32,40] and short-range [41] reactions. The effective reaction order depends again on the spatial dimensionality and on the transfer rate type [40].

Presently, the influence of the support on the kinetics behavior of the one-species annihilation reaction is still a topic of concern in the literature [42–44], in catalytic activated reactions [45,46] or in reaction-diffusion processes taking place on scale-free networks [47], for example. However, the effect of the reaction kinetics itself has not been dealt with in depth. A few results concern diffusion-controlled transient reactions, for which it has been proven that the influence of the probability of reaction on kinetics may be negligible at

sufficiently long times [48–50]. The conclusion was confirmed when Martín *et al.* [51] found the steady-state density of particles as a function of the reaction probability and the input rate in the one-dimension steady state. A study on the explicit dependence of fluctuations on reaction kinetics becomes necessary, especially when the CFD reaction is embedded within a complex reaction scheme, as it happens in the model defined by Eqs. (1), (2), and (5), or in other surface processes on heterogeneous catalysts [52,53], for example. Successful encounters between active particles and, consequently, the reaction rate of the annihilation reaction, do depend on how those same particles are affected by other coupled reactions, i.e., by their reaction rates.

We analyze here the reactant self-ordering and the rate law of the CFD reaction when it is coupled to an adsorption reaction (1) and competes with a monomolecular desorption reaction (2). This problem is particularly relevant in order to understand anomalies in the reaction order of the CFD, as assessed in the hydrogen desorption reaction from H-terminated silicon surfaces. As we are strictly interested in the influence of the overall reactive kinetics on fluctuations, we shall avoid the shadowing effect of diffusion by assuming a temperature below that required for surface diffusion and A particles are accordingly immobile. We shall show that the reaction schemes (1), (2), and (5), defined on a one-dimensional support, generate local spatial fluctuations of the particle density that ultimately determine a fractional reaction order for the CFD reaction under the steady-state conditions. These fluctuations result in a nonequilibrium steady-state heterogeneous spatial distribution of particles, involving either a local enhancement in the occupancy of vacant sites around the particles—reaction is then faster than predicted by the MFA—or, alternatively, a local depletion—reaction slows down with respect to the MFA—depending on the reactive parameters of the model. This is a surprising result inasmuch as a spontaneous aggregation of particles, as a result of the local enrichment in A particles, is not expected in the case of the $A+A \rightarrow 0$ reaction, although it has been observed in reaction-diffusion processes on scale-free networks [47]. Our aim is to explore quantitatively the nature of such correlations and to show that, although they are induced by the CFD reaction, they indeed depend on the overall reaction kinetics. In a previous publication [54], we investigated qualitatively the limits of validity of the MFA in the context of electrochemistry under conditions of hindered surface mobility of adsorbates. Simulations showed that the CFD reaction obeys a fractional order kinetics. The system approached monotonously the MFA dynamics as the number of interacting neighbors was increased. This was achieved by increasing the coordination number or by raising the dimensionality.

The paper is structured as follows. We shall start by showing results of microscopic Monte Carlo simulations that support a steady-state anomalous order kinetics in the CFD reaction (Sec. II). In Sec. III the dynamics of the next neighbors (nn) correlations will be analyzed and a closed-analytical expression for the reaction order will be obtained as function of the kinetic parameters of the model, fitting with great accuracy the results of numerical microscopic simulations. Three different regimes are observed, leading to

values of the reactive order that are higher, equal, and lower than the MFA standard value of 2. Steady-state correlations will be studied in Sec. IV. The spatial decay of correlations is found to be short ranged, which is in turn a consequence of the short-range nature of the reaction dynamics. By means of the g-approximation [55] we find the explicit dependence of spatial correlations on the kinetic constants. The analytic approach shows an excellent agreement with simulation results. We conclude in Sec. V.

II. MICROSCOPIC SIMULATION AND RESULTS

The scheme given by reactions (1), (2), and (5) is microscopically studied by Monte Carlo simulations on a one-dimensional (1D) lattice of L sites with periodic boundary conditions. Each lattice site may be either empty (state S) or occupied by a single particle A (state A). Starting from a uniform configuration in which all sites of the lattice are empty, the simulation proceeds at each Monte Carlo step by randomly selecting a lattice site. Then a random number, $\text{rnd} \in [0, 1]$, is generated and the state of the cell is computed according to the following rules.

(1) If the chosen lattice site is empty, then adsorption reaction (1) occurs if $\text{rnd} \in [0, k_1[$. The site is then filled with an A particle.

(2) If, on the contrary, the site is already in state A , two transitions for the state of the cell are possible:

(2a) If $\text{rnd} \in [0, k_2[$ the particle A desorbs through reaction (2) and the state of the site changes from A to S .

(2b) If $\text{rnd} \in [k_2, k_2+k_3[$, one of the two nearest neighbors of the site is then randomly chosen and checked. If it is occupied by another particle A , then cooperative reaction (5) proceeds and the two A particles desorb leaving their sites empty in state S .

(3) If no reaction occurs, the site remains unchanged.

At the end of each Monte Carlo step, discrete time t is increased by Δt . By taking the time step length $\Delta t=1/L$, we ensure that all lattice sites are likely to be visited on average once per unit time, $t=1$.

After a given time τ , the system reaches a steady state characterized by a steady-state particle coverage fraction $\bar{\vartheta}$ that depends on the reaction parameters of the model $\{k_i\}$ though not on the initial state. Simulations show that steady-state values and correlations are invariant under isotropic scale transformations of the set of kinetic constants $\{k_1, k_2, k_3\} \rightarrow \{bk_1, bk_2, bk_3\}$. This will be supported by the theoretical analysis developed in the next section. The number of independent parameters of the model can accordingly be cut to two: $\{K_1, K_2, 1\}$, where $K_1=k_1/k_3$ and $K_2=k_2/k_3$. Parameter K_1 typifies the adsorption-desorption route consisting of the monomolecular adsorption and the CFD—steps (1) and (5)—while K_2 quantifies the relative importance of the two competing desorption steps, (2) and (5).

Monte Carlo simulations supply a value for $\bar{\vartheta}$ and the steady-state CFD reaction rate \bar{R}_{CFD} , defined as the average number of particles that desorb through the CFD reaction per units of length and time under steady-state conditions. The effective reaction order of the CFD, α , is then obtained by

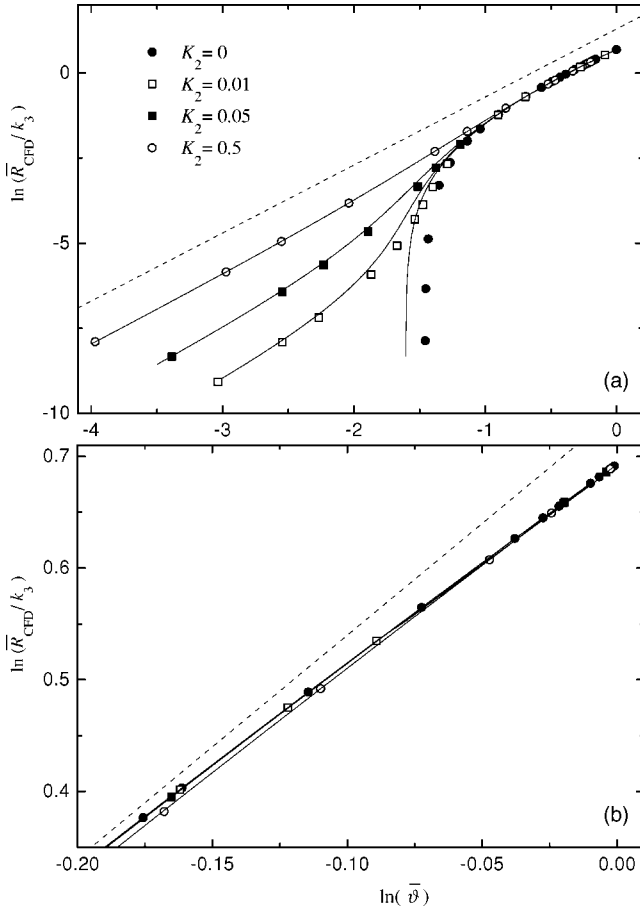


FIG. 1. (a) In logarithmic scale, the steady state, rescaled CFD reaction rate, \bar{R}_{CFD}/k_3 vs steady-state coverage of particles, $\bar{\vartheta}$, obtained varying K_1 for different values of K_2 . Symbols correspond to results obtained from simulations while continuous lines stand for the analytical approach (21). The dotted line with slope 2 indicates the second order reaction kinetics predicted by the mean field approach. (b) Zoom at high coverage values.

fitting simulation data to the expression $\bar{R}_{\text{CFD}} \propto \bar{\vartheta}^\alpha$. In the case of the classical chemical kinetics, the order 2 is expected. Figure 1 displays the results for this relationship as obtained from simulations (symbols) of a $L=10^5$ lattice. Each curve corresponds to a fixed value of K_2 and has been obtained by varying K_1 —this particular parameter choice will become apparent in the theoretical analysis of Sec. III. Actual values of $\{k_1, k_2, k_3\}$ have been chosen arbitrarily in order to sample the entire parameter space. Departure from second order kinetics (dotted line) is especially significant in the small K_2 range and the MFA limit is approached everywhere by raising K_2 . Understandably, a dominating monomolecular desorption (high K_2) shadows the effects of an anomalous CFD kinetics. On the other hand, when K_2 is small deviations from second-order kinetics are more pronounced in the low coverage range (attained for $K_1 \ll 1$), reaching effective reaction orders much larger than 2. As coverage increases (larger K_1) figures display an effective reaction order slightly smaller than two (see enlargement in box) and all curves seem to collapse into a single limiting behavior as we approach full adsorbate coverage. We shall

show in Sec. III that there is no universal behavior here: an actual dependence of the effective reaction order on K_2 does exist in the limit $\bar{\vartheta} \rightarrow 1$, though it induced differences that are hardly noticeable in Fig. 1. We shall prove in Sec. III that Fig. 1 is universal for this model, i.e., it does not depend on the particular values of $\{k_i\}$ used in simulations, once \bar{R}_{CFD} is appropriately rescaled with k_3 .

The anomalous reaction order can be better assessed by invoking the following correction to the standard, macroscopic rate equation:

$$\frac{d\vartheta}{dt} = k_1(1 - \vartheta) - k_2\vartheta - 2k_3\vartheta P, \quad (6)$$

with $\vartheta(0) = \vartheta_0$ as initial conditions ($\vartheta_0 = 0$ in our simulations). The first two contributions to Eq. (6) are usual for steps (1) and (2), respectively. The function $P(t)$ represents the average fraction of reactants around an A particle, that is, its *active neighborhood* (AN). The MFA extends the AN to the whole lattice: $P(t) = \vartheta(t)$, thus justifying a second order term. Here, the low-dimensionality of the lattice, combined with the absence of diffusion and short-range interactions, generates fluctuations of the particle density in the AN that lead to deviations from the MFA: $P(t) \neq \vartheta(t)$. Such deviations will be characterized by the parameter γ , defined as

$$\gamma(t) = \frac{\ln P(t)}{\ln \vartheta(t)}. \quad (7)$$

The CFD rate then takes the form

$$R_{\text{CFD}}(t) = 2k_3\vartheta^{\gamma(t)+1}(t). \quad (8)$$

The exponent $\gamma(t)$ amounts to a reaction order containing all the information about the density fluctuations in the AN. Any deviation of γ from 1 implies an inhomogeneous distribution of A particles on the lattice. The range $\gamma > 1$ represents a local density around A particles smaller than that indicated by the homogeneous coverage fraction value, ϑ . We shall refer to it as “local dispersion.” On the contrary, if $\gamma < 1$, the density of occupied sites around A particles is larger than that expected from the homogeneous coverage fraction value ϑ , and we have “local aggregation.”

We plot in Fig. 2 the steady-state values for γ for different values of the normalized constants, K_1 and K_2 . Symbols identify results from simulations. The reaction order $\bar{\gamma}$ is obtained by averaging from Eq. (7) the local density around each particle under steady-state conditions. Results illustrate the fact that the exact MFA value, $\bar{\gamma} = 1$, is the exception.

Three different ranges can be inferred from Fig. 2:

$$\bar{\gamma} \begin{cases} > 1 & \text{if } (K_1 - K_2) < 1, \\ = 1 & \text{if } (K_1 - K_2) = 1, \\ < 1 & \text{if } (K_1 - K_2) > 1, \end{cases} \quad (9)$$

which correspond, according to simulations, to the following coverage values:

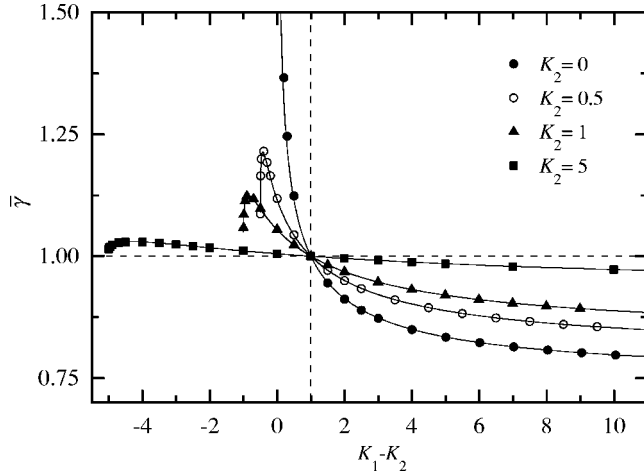


FIG. 2. Steady-state reaction order, $\bar{\gamma}$, vs $K_1 - K_2$ for different values of K_2 . Scattered points correspond to results from simulations while continuous lines stand for the analytical approach given in Eqs. (18)–(20).

$$\bar{\gamma} \begin{cases} > 1 & \text{if } \bar{\vartheta} < 0.5, \\ = 1 & \text{if } \bar{\vartheta} = 0.5, \\ < 1 & \text{if } \bar{\vartheta} > 0.5. \end{cases} \quad (10)$$

If $\bar{\gamma} > 1$, the active neighborhood, $\bar{P} \approx [\bar{\vartheta}]^{\bar{\gamma}}$, is smaller than the average coverage fraction, $\bar{\vartheta}$, which is to be interpreted in terms of a smaller probability of occurrence of pairs of adjacent A particles than under a randomly covered lattice. The contrary occurs when $\bar{\gamma} < 1$ and we shall understand that we shall find, on average, more pairs of A particles than expected under an homogeneous distribution of the coverage. Attraction or repulsion forces between adsorbed particles and surface mobility cannot be responsible for any aggregation or dispersion because we have precluded any explicit interaction. They can be only understood as an indirect effect of the kinetics of our model reaction. Case $\bar{\gamma} > 1$ is obtained when $K_1 - K_2 < 1$ ($k_1 < k_2 + k_3$). For this relation between the kinetic constants we have $\bar{\vartheta} < 0.5$. If by chance any particle aggregate is formed, it disintegrates under the action of a fast CFD reaction, with an ensuing little chance of being reconstituted by the slow and spatially random adsorption (1). This leads to an effective “dispersion” of adsorbed particles for which the likelihood for CFD reaction is severely reduced, yielding a smaller rate than that predicted by the MF approach: $\bar{\vartheta}^{\bar{\gamma}+1} < \bar{\vartheta}^2$. On the contrary, when $K_1 - K_2 > 1$ ($k_1 > k_2 + k_3$), $\bar{\gamma} < 1$ and a few vacant sites appear on the surface ($\bar{\vartheta} > 0.5$). These vacant sites will be filled under the action of the adsorption reaction (1). On the other hand, each occasional successful CFD transition will create two contiguous vacant sites leading to an “aggregation” of vacant sites, which entails, correspondingly, that of A particles. This aggregation effect “favors” the CFD reaction $\bar{\vartheta}^{\bar{\gamma}+1} > \bar{\vartheta}^2$. In both cases, the effects are smoothed out when K_2 increases. The monomolecular desorption (2) tends to thwart the establishment of correlations, thus making the particle distribution

homogeneous. This is observed in Fig. 2: as K_2 increases, $\bar{\gamma} \rightarrow 1$ for all K_1 . Finally, the value $\bar{\gamma} = 1$ is also trivially recovered when inhibiting the CFD reaction, i.e., when $k_3 = 0$.

III. THEORETICAL ANALYSIS

Our aim in this section is to develop a model that predicts the dependence of the reaction order on the kinetics parameters as shown in Fig. 2. By doing this, we shall also obtain the stationary value of other observables, such as the particles density or the reaction rates. We start by studying the dynamics of the active neighborhood $P(t)$. We introduce a Heaviside indicator function for the occupation of a cell:

$$\sigma_i = \begin{cases} 1, & \text{if site } i \text{ is occupied by an } A \text{ particle} \\ 0, & \text{otherwise.} \end{cases}$$

For a given configuration $\{\sigma\} = (\sigma_1 \cdots \sigma_L)$ at time t , the density of particles $\vartheta(\{\sigma\}; t)$ is

$$\vartheta(\{\sigma\}; t) = L^{-1} \sum_{i=1}^L \sigma_i, \quad (11)$$

and the AN, $P(\{\sigma\}; t)$, is given by

$$P(\{\sigma\}; t) = \left(\sum_{i=1}^L \sigma_i \right)^{-1} \sum_{i=1}^L \left(\frac{1}{2} \sigma_i (\sigma_{i+1} + \sigma_{i-1}) \right). \quad (12)$$

We can average Eqs. (11) and (12) over all configurations $\{\sigma\}$ and assume translational invariance from here on, i.e., in the limit $L \rightarrow \infty$ there are no privileged sites in the lattice. Then we have $\langle \sigma_i \rangle = \langle \sigma_j \rangle = \vartheta(t)$ and $\langle \sigma_i \sigma_{i+1} \rangle = \langle \sigma_j \sigma_{j+1} \rangle = C_2(t)$ for all i, j , where $C_2(t)$ is the two-particle correlation. Thus we can write from Eq. (12)

$$C_2(t) = \vartheta(t) P(t). \quad (13)$$

Let us introduce now the n -particle correlation $C_n(t) = \langle \sigma_i \sigma_{i+1} \cdots \sigma_{i+n-1} \rangle$, which stands for the probability to find at time t a chain of n adjacent A -particles. Its time evolution is determined exactly by the following differential equation:

$$\frac{dC_n}{dt} = k_1 \sum_{j=i}^{i+n-1} \langle \sigma_i \cdots \sigma_{j-1} (1 - \sigma_j) \sigma_{j+1} \cdots \sigma_{i+n-1} \rangle - nk_2 C_n - k_3(n-1)C_n - 2k_3 C_{n+1}. \quad (14)$$

The first term in Eq. (14) is the probability of formation of a chain from an incomplete chain of n sites with an empty site—adsorption reaction (1). The second term gives the probability of breaking the chain of n particles with the desorption of one of them via reaction (2). The third term stands for the probability of reaction of one of the $(n-1)$ A - A pairs of the n -chain through the CFD reaction. The fourth considers the possibility of the CFD reaction between the particles at the ends of the chain and an adjacent site.

For $n=1$, $C_1(t)$ gives the averaged occupation probability per lattice site, i.e., the global density of particles, and Eq. (6) is recovered from Eq. (14). For $n=2$ we obtain

$$\frac{dC_2}{dt} = 2k_1 \vartheta(1 - P) - (2k_2 + k_3) \vartheta P - 2k_3 C_3. \quad (15)$$

We can break down now $C_3(t)$ by assuming spatial Markovianity [56]

$$\text{Prob}(\sigma_i, \sigma_{i+1}, \sigma_{i+2}) = \text{Prob}(\sigma_i, \sigma_{i+1})\text{Prob}_c(\sigma_{i+2}|\sigma_{i+1}), \quad (16)$$

i.e., we have considered that the probability for $\sigma_{i+2}(t)$ depends only on the value $\sigma_{i+1}(t)$ in the nearest cell and not on that in other cells further away. This assumption is a direct consequence of precluding interactions beyond first neighbors, which is the case in the present model. It has been proved to be valid in the problem of immobile annihilating reactants without input of particles [36–39]. There, it was shown that the ansatz $C_n(t) = \vartheta(t)P^{n-1}(t)$ helps in solving the coupled hierarchy of equations for the dynamics of clusters containing contiguous A -particles, and thereby obtaining the exact solution found in [35].

Following this assumption, the three-particle correlation takes the form

$$C_3(t) = \sum_{\sigma_i} \sum_{\sigma_{i+1}} \sum_{\sigma_{i+2}} (\sigma_i \sigma_{i+1} \sigma_{i+2}) \text{Prob}(\sigma_i, \sigma_{i+1}, \sigma_{i+2}) = \vartheta(t)P^2(t), \quad (17)$$

where we have made use of the fact that $\text{Prob}(\sigma_j=1)$ is simply $\vartheta(t)$ and $\text{Prob}_c(\sigma_{j+1}=1|\sigma_j=1) = P(t) \forall j$. Equation (17) retrieves the generic ansatz proposed in Ref. [36] for $n=3$, consistently with the reaction model that precludes long-range interactions.

By replacing $C_3(t)$ in Eq. (15) with the approximation obtained in Eq. (17), and considering steady-state conditions,

we obtain the kinetic parameters dependence of the stationary value of $P(t)$

$$\bar{P} = \frac{1}{4}(-1 - 2K_1 - 2K_2 + \{(2K_1 + 2K_2 + 1)^2 + 16K_1\}^{1/2}). \quad (18)$$

The steady-state particle coverage obtained from Eq. (6) takes the following form:

$$\bar{\vartheta} = \frac{2K_1}{\{(2K_1 + 2K_2 + 1)^2 + 16K_1\}^{1/2} - 1}. \quad (19)$$

In the limit of small input of particles ($K_1 \rightarrow 0$), and for $K_2 = 0$, Eq. (19) yields the same asymptotic steady-state coverage, $\bar{\vartheta} = 0.2$, of Ref. [41].

By recalling definition (7), the parameter dependence of the reaction order under steady-state conditions is immediately obtained by substituting Eqs. (18) and (19) into

$$\bar{\gamma} \approx \frac{\log \bar{P}}{\log \bar{\vartheta}}. \quad (20)$$

Both the reaction order (20) and the steady-state coverage value (19) do only depend on rescaled parameters K_1 and K_2 , hence substantiating the prior claim made in Sec. II. We finally recover the dependence of \bar{R}_{CFD} on $\bar{\vartheta}$. We first produce, from Eq. (19), K_1 as a function of $\bar{\vartheta}$ and K_2 , and then make use of the expression $\bar{R}_{\text{CFD}} \approx 2k_3 \bar{\vartheta} \cdot \bar{P}$, together with Eqs. (18) and (19), in order to get \bar{R}_{CFD}/k_3 in terms of $\bar{\vartheta}$ and K_2

$$\frac{\bar{R}_{\text{CFD}}}{k_3} \approx f(\bar{\vartheta}, K_2) = \frac{\bar{\vartheta}(-1 - 2K_2 + 5\bar{\vartheta} + \{4K_2^2 + (1 - 5\bar{\vartheta})^2 + 4K_2(1 - \bar{\vartheta} + 4\bar{\vartheta}^2)\}^{1/2})}{2(1 + \bar{\vartheta})}. \quad (21)$$

Notice that \bar{R}_{CFD} has been rescaled in Eq. (21). In a log-log scale this amounts to an additive constant which moves figures up or down. For a negligible CFD rate compared to the monomolecular desorption rate, Eq. (21) behaves as

$$f(\bar{\vartheta}, K_2) \sim \bar{\vartheta}^2, \quad K_2 \gg 1, \quad (22)$$

and we retrieve the MFA value. On the other hand,

$$f(\bar{\vartheta}, K_2) \sim \bar{\vartheta}^{[(4K_2+7)/(2K_2+2)]}, \quad \bar{\vartheta} \rightarrow 1, \quad (23)$$

with an exponent valuing 1.75 for $K_2=0$ and saturating at 2 for relatively large K_2 . No universal scaling can be thus associated to curves on Fig. 1. On the basis of Eqs. (22) and (23) we expect at low coverage values a scaling behavior for each K_2 , crossing over into a uniform scaling behavior only for large coverage and large K_2 .

Predictions from Eqs. (21) and (18)–(20) are drawn with a solid line in Figs. 1 and 2, respectively. Agreement between simulations and analytical calculations is perfect except for the CFD rate at value $K_2=0$ in the limit of a very small input of particles: $K_1 \rightarrow 0$ and $\bar{\vartheta} \ll 1$, see Fig. 1.

IV. SPATIAL CORRELATIONS IN THE STEADY STATE

Up to now, we have limited the study to first neighbors (nn) correlations because they are responsible for the failure of the MF approach. These local correlations have been captured in the fractional reaction order $1 + \bar{\gamma}$. Our purpose now is to study the spatial decay of particle correlations as well as its dependence on the model parameters K_1 and K_2 .

Due to translational invariance correlations depend only on the distance between sites. The time evolution of the pair-

correlation function $\Gamma_n(t) = \langle \sigma_i \sigma_j \rangle$, where $n = |j - i|$, is given for $n > 1$ by

$$\begin{aligned} \frac{d}{dt} \Gamma_n = & k_1 [\langle (1 - \sigma_i) \sigma_j \rangle + \langle \sigma_i (1 - \sigma_j) \rangle] - k_2 [\langle \sigma_i \sigma_j \rangle + \langle \sigma_i \sigma_j \rangle] \\ & - \frac{1}{2} k_3 [\langle \sigma_{i-1} \sigma_i \sigma_j \rangle + \langle \sigma_{i-1} \sigma_i \sigma_j \rangle + \langle \sigma_i \sigma_{i+1} \sigma_j \rangle \\ & + \langle \sigma_i \sigma_{i+1} \sigma_j \rangle + \langle \sigma_i \sigma_{j-1} \sigma_j \rangle + \langle \sigma_i \sigma_{j-1} \sigma_j \rangle + \langle \sigma_i \sigma_j \sigma_{j+1} \rangle \\ & + \langle \sigma_i \sigma_j \sigma_{j+1} \rangle], \end{aligned} \quad (24)$$

where sites chosen for reaction are indicated with a bold, underlined subscript. The term in Eq. (24) multiplied by k_1 stands for the probability of creation of correlation between position i and j with the occupation of an empty site via adsorption (1); the term multiplied by k_2 gives the probability of destruction of the correlation with the desorption of one of the two particles—reaction (2)—while the term multiplying k_3 stands for the destruction of correlations through the CFD reaction between one of the particles at position i or j and any of their first neighbors.

According to the occupation function σ_i defined in Sec. III, the trivial case $i = j$ gives $\Gamma_0(t) = \vartheta(t)$. Case $n = 1$ deserves special attention because if $j = i + 1$, both terms $\langle \sigma_i \sigma_{i+1} \sigma_{i+1} \rangle$ and $\langle \sigma_i \sigma_{i+1} \rangle$ in Eq. (24) represent the same transition between selected site i and its neighbor $i + 1$. The same holds for $\langle \sigma_i \sigma_{i+1} \sigma_{i+1} \rangle$ and $\langle \sigma_i \sigma_{i+1} \rangle$. By suppressing one of them in Eq. (24), we get

$$\begin{aligned} \frac{d}{dt} \Gamma_1 = & k_1 [\langle (1 - \sigma_i) \sigma_{i+1} \rangle + \langle \sigma_i (1 - \sigma_{i+1}) \rangle] - k_2 [\langle \sigma_i \sigma_{i+1} \rangle \\ & + \langle \sigma_i \sigma_{i+1} \rangle] - \frac{1}{2} k_3 [\langle \sigma_{i-1} \sigma_i \sigma_{i+1} \rangle + \langle \sigma_{i-1} \sigma_i \sigma_{i+1} \rangle \\ & + \langle \sigma_i \sigma_{i+1} \sigma_{i+1} \rangle + \langle \sigma_i \sigma_{i-1} \sigma_{i+1} \rangle + \langle \sigma_i \sigma_{i+1} \sigma_{i+2} \rangle \\ & + \langle \sigma_i \sigma_{i+1} \sigma_{i+2} \rangle]. \end{aligned} \quad (25)$$

In the thermodynamic limit $L \rightarrow \infty$, $\Gamma_1(t) = C_2(t)$ and Eq. (15) is recovered from Eq. (25). By introducing the three-particle correlation function $H_{i,j,k}(t) = \langle \sigma_i \sigma_j \sigma_k \rangle$, we can write for Eq. (24)

$$\begin{aligned} \frac{d}{dt} \Gamma_n = & 2k_1 \vartheta - 2k_1 \Gamma_n - 2k_2 \Gamma_n - k_3 (H_{i-1,i,i+n} + H_{i,i+1,i+n} \\ & + H_{i,i+n-1,i+n} + H_{i,i+n,i+n+1}), \end{aligned} \quad (26)$$

with $n > 1$. At the steady state, we have

$$\begin{aligned} 2K_1 (\bar{\vartheta} - \bar{\Gamma}_n) - 2K_2 \bar{\Gamma}_n = & \bar{H}_{i-1,i,i+n} + \bar{H}_{i,i+1,i+n} + \bar{H}_{i,i+n-1,i+n} \\ & + \bar{H}_{i,i+n,i+n+1}. \end{aligned} \quad (27)$$

In order to study the spatial decay of the two-particle correlations at steady state, i.e., the dependence of $\bar{\Gamma}_n$ on n , we introduce the fluctuation correlation function

$$f_n(t) = \langle \delta \sigma_i \delta \sigma_j \rangle, \quad (28)$$

with $\delta \sigma_i = \sigma_i - \langle \sigma \rangle$ and $\langle \sigma \rangle = \vartheta(t)$. Thus

$$\Gamma_n(t) = \vartheta^2(t) + g_n(t) [\vartheta(t) - \vartheta^2(t)], \quad (29)$$

with $g_n(t) = f_n(t) / \langle (\delta \sigma)^2 \rangle$.

To break down the three-particle correlation functions appearing in Eq. (27) we shall make use of two approximations. First, the so-called ‘‘g-approximation’’ [55], which predicts the following for the conditional average:

$$\langle \sigma_j | \sigma_i \rangle = \sum_{\sigma_j} \sigma_j \text{Prob}(\sigma_i, \sigma_j) = [\langle \sigma \rangle + g_n (\sigma_i - \langle \sigma \rangle)] \text{Prob}(\sigma_i). \quad (30)$$

It can be interpreted as a linearization of correlations about the zeroth-order (MF) approximation, which neglects any correlation: $\langle \sigma_j | \sigma_i \rangle = \langle \sigma \rangle \text{Prob}(\sigma_i)$. This approach has been used in previous works on trimolecular reactive systems to calculate analytically the values of the fluctuation correlations, yielding a very good agreement with simulations [57]. From the following definition of $\langle \sigma_i \sigma_j \rangle$:

$$\langle \sigma_i \sigma_j \rangle = \sum_{\sigma_i} \sum_{\sigma_j} \sigma_i \sigma_j \text{Prob}(\sigma_i, \sigma_j) = \sum_{\sigma_i} \sigma_i \langle \sigma_j | \sigma_i \rangle, \quad (31)$$

Eq. (29) is easily recovered by using Eq. (30).

The second approximation is to assume again spatial Markovianity in order to decouple three-point probabilities, as in Eq. (16). Then, we can write for $\bar{H}_{i-1,i,i+n}$

$$\begin{aligned} \bar{H}_{i-1,i,i+n} = & \sum_{\sigma_{i-1}} \sum_{\sigma_i} \sum_{\sigma_{i+n}} \sigma_{i-1} \sigma_i \sigma_{i+n} \text{Prob}(\sigma_{i-1} \sigma_i \sigma_{i+n}) \\ = & \sum_{\sigma_{i-1}} \sum_{\sigma_i} \sum_{\sigma_{i+n}} \sigma_{i-1} \sigma_i \sigma_{i+n} \text{Prob}(\sigma_{i-1} \sigma_i) \frac{\text{Prob}(\sigma_i \sigma_{i+n})}{\text{Prob}(\sigma_i)} \\ = & \sum_{\sigma_{i-1}} \sum_{\sigma_i} \sigma_{i-1} \sigma_i \text{Prob}(\sigma_{i-1} \sigma_i) [\langle \sigma \rangle + \bar{g}_n (\sigma_i - \langle \sigma \rangle)] \\ = & \bar{\Gamma}_1 \bar{\vartheta} + \bar{g}_n \sum_{\sigma_i} \sigma_i^2 \langle \sigma_{i-1} | \sigma_i \rangle - \bar{g}_n \bar{\Gamma}_1 \bar{\vartheta} \\ = & \bar{\Gamma}_1 \bar{\vartheta} + \bar{g}_n (\bar{\vartheta}^2 + \bar{g}_1 \bar{\vartheta} - \bar{g}_1 \bar{\vartheta}^2) - \bar{g}_n \bar{\Gamma}_1 \bar{\vartheta}. \end{aligned} \quad (32)$$

First neighbor correlation in the steady state, $\bar{\Gamma}_1$, is obtained from the steady-state condition of Eq. (6), provided $\bar{\Gamma}_1 = \bar{C}_2 = \bar{\vartheta} \cdot \bar{P}$,

$$\bar{\Gamma}_1 = \frac{K_1 (1 - \bar{\vartheta}) - K_2 \bar{\vartheta}}{2}. \quad (33)$$

Substituting Eqs. (33) and (29) in Eq. (32) we get

$$\bar{H}_{i-1,i,i+n} = \bar{\Gamma}_n \frac{K_1 - \bar{\vartheta} (K_1 + K_2)}{2 \bar{\vartheta}}. \quad (34)$$

By doing the same with the other three \bar{H} terms in Eq. (27) we get $\bar{H}_{i,i+n,i+n+1} = \bar{H}_{i-1,i,i+n}$ and

$$\bar{H}_{i,i+1,i+n} = \bar{H}_{i,i+n-1,i+n} = \bar{\Gamma}_{n-1} \frac{K_1 - \bar{\vartheta} (K_1 + K_2)}{2 \bar{\vartheta}}. \quad (35)$$

Finally, by substituting Eqs. (34) and (35) in Eq. (27) we obtain the following recursive relation:

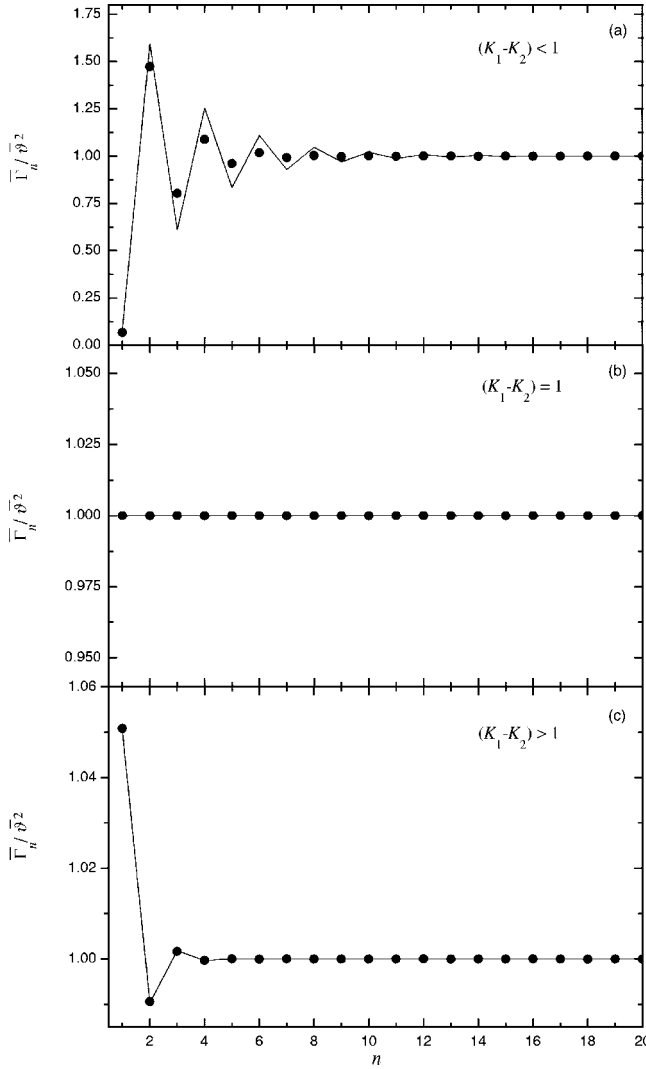


FIG. 3. Spatial decay of the normalized pair-correlation function at the steady state, $\bar{\Gamma}_n / \bar{\vartheta}^2$, for three different set of kinetic constants: (a) $K_1=0.01, K_2=0$; (b) $K_1=2, K_2=1$; and (c) $K_1=3, K_2=0$. Solid points correspond to results from simulations while continuous lines stand for the approach given in Eq. (36), with $\bar{\Gamma}_1$ obtained from Eq. (33) using Eq. (19).

$$\bar{\Gamma}_n = \bar{\Gamma}_{n-1} \left(\frac{-K_1 + \bar{\vartheta}(K_1 + K_2)}{K_1 + \bar{\vartheta}(K_1 + K_2)} \right) + \frac{2K_1\bar{\vartheta}^2}{K_1 + \bar{\vartheta}(K_1 + K_2)} \quad (36)$$

for $n > 1$. By using Eq. (19) in Eq. (33), explicit dependence of $\bar{\Gamma}_1$ on K_1 and K_2 is obtained. Thus spatial decay of correlations at steady state is perfectly determined from Eq. (36) without resorting to simulations.

We show in Fig. 3 an example of the spatial decay of the normalized pair correlation function at steady state, $\bar{\Gamma}_n / \bar{\vartheta}^2$, for each kinetic regime (9). Points represent results from simulations and continuous lines the dependence of $\bar{\Gamma}_n$ on n from Eq. (36). Figure 3(a) illustrates the “local dispersion” regime, in which particles show a tendency to occupy every

other site: first neighbor correlation is smaller than 1 ($\bar{\Gamma}_1 < \bar{\vartheta}^2$), indicating that the probability to have two neighboring particles is smaller than that predicted by the MF approach. Figure 3(b) is an example of the MF regime in which kinetics lead to an uncorrelated distribution of particles: $\bar{\Gamma}_n = \bar{\vartheta}^2$ for all n . Finally, Fig. 3(c) illustrates the “local aggregation” regime that also shows an alternating distribution of particles: now $\bar{\Gamma}_1 > \bar{\vartheta}^2$ and particles have a higher probability of having neighbor sites occupied. The agreement between simulations and the analytical approach given in Eq. (36) is very good.

It can also be easily proved from Eqs. (36) and (29) that

$$\bar{g}_n = \bar{g}_{n-1} \left(\frac{-K_1 + \bar{\vartheta}(K_1 + K_2)}{K_1 + \bar{\vartheta}(K_1 + K_2)} \right). \quad (37)$$

As the fluctuation correlation function is directly related to \bar{g}_n by means of $\bar{f}_n = \bar{g}_n(\bar{\vartheta} - \bar{\vartheta}^2)$, the independence from n of the factor that multiplies \bar{g}_{n-1} in Eq. (37) predicts an exponential decay of the fluctuations correlations with n and, consequently, short-ranged correlations, as obtained in simulations. A similar exponential decay of \bar{f}_n was obtained in the trimolecular case studied in [57].

V. DISCUSSION

In some circumstances the cooperative full desorption reaction is coupled to other reactions involving A particles. We have thus considered the combination of the CFD with a random decomposition, on a one-dimensional regular lattice. Adsorbed particles are immobile until they react and desorb. The lattice is in contact with a reservoir of particles thus making possible the establishment of steady-state conditions. This is a lumped model covering the final steps leading to desorption of molecular hydrogen on H-terminated silicon surfaces. Active particles are single occupied dimers (SOD) that prepare to form double occupied dimers. Empty sites are clean substrate dimers.

In the absence of the competitor random H atom transfer reaction, next neighbors pairings of immobile particles in the CFD reaction introduce correlations, which in turn convey anomalies in its reaction order in terms of a significant departure from the MFA value of 2. Underneath these attributes we discover that particles can be found in the form of aggregates or, alternatively, be evenly distributed along the lattice. This interesting feature has already been reported for trimolecular reactions [57], with correlations dependent exclusively on initial conditions. Here, we show that this self-ordering can be extended to bimolecular reactions, although here correlations are instead dependent on kinetic parameters. Particles are dispersed in the regime limited by SOD formation because the eventual creation of pairs of active neighbors is offset by the CFD reaction. Lattice coverage is low and the CFD reaction is slowed down by a reaction order larger than two. At the other end, in the CFD-limited mechanism the probability for a particle of having first neighbors is high. Consequently, lattice coverage is also high and occasional CFD desorptions create pairs of contiguous vacancies

that indirectly contribute to pack together occupied sites. The phenomenon is therefore characterized by a low reaction order and, consequently, a faster CFD rate than that predicted by the MFA. It is not surprising to find these effects mitigated by the inclusion of an alternative SOD sink route involving single particle events. The process $A \rightarrow S$ competes with the CFD and, in becoming dominant, can eventually overshadow CFD anomalies and drive the system close to the MFA predictions.

Interestingly, some of the present theoretical results encompass some experimental findings in the hydrogen evolution reaction on silicon. Near first order kinetics is found at moderate to high coverage [4,12,13] modified to near second order for low coverage [4]. This is the trend observed in Fig. 2 for the range $K_1 > K_2$, that is step (1) dominating over step (2). The behavior is especially noticeable for $K_2=0$ —negligible hydrogen mobility, for example—where the system displays near first order kinetics at high coverage (large K_1), approaching second order as coverage is reduced to more moderate values (decreasing K_1). The transition is curbed for larger K_2 values. A shift toward a reaction order

slightly larger than two is predicted here for further coverage dwindling. Except for the case of low K_2 these deviations may well fall within experimental errors. Alternatively, the range of small values of K_1 can be attained with a fast pre-pairing, i.e., large k_3 , that is a fast overall desorption rate, which is achieved for temperatures over the β_2 desorption peak [4]. Here, hydrogen mobility is enhanced and consequently we may well be confronted with a situation where k_2 moves toward k_3 : we get a rising value for K_2 and thus a reaction order close to two.

It is noteworthy that we find shifting reaction order in the static bimolecular annihilation reaction. The model is a very simplistic view of what is under consideration in the case of hydrogen evolution on H-terminated silicon. Important features such as the thermal surface diffusion, alternative dimer recombination routes for desorption or a rate-limiting desorption from DOD, and hydrogen passivation (low temperatures) have been disregarded. Nevertheless, it points at the fact that the CFD reaction may well account itself for the desorption rate anomalies reported in the literature.

-
- [1] J. M. Ripalda, A. Khatiri, T. J. Kryzewski, J. D. Gale, and T. S. Jones, *Phys. Rev. B* **68**, 073311 (2003).
- [2] F. M. Zimmermann and X. Pan, *Phys. Rev. Lett.* **85**, 618 (2000).
- [3] C. Filippi, S. B. Healy, P. Kratzer, E. Pehlke, and M. Scheffler, *Phys. Rev. Lett.* **89**, 166102 (2002).
- [4] M. Dürr, Z. Hu, A. Biedermann, U. Höfer, and T. F. Heinz, *Phys. Rev. Lett.* **88**, 046104 (2002).
- [5] T. R. Bramlett, Q. Lu, T. Karasawa, M. A. Hasan, S. K. Jo, and J. E. Greene, *J. Appl. Phys.* **76**, 1884 (1994).
- [6] P.-H. Wu and D.-S. Lin, *Phys. Rev. B* **57**, 12421 (1998).
- [7] T. Ohira, O. Ukai, and M. Noda, *Surf. Sci.* **458**, 216 (2000).
- [8] R. W. Price, E. S. Tok, and J. Zhang, *J. Cryst. Growth* **209**, 306 (2000).
- [9] H. Nakazawa and M. Suemitsu, *Appl. Surf. Sci.* **130–132**, 298 (1998).
- [10] H. Nakazawa, M. Suemitsu, and N. Miyamoto, *Surf. Sci.* **465**, 177 (2000).
- [11] U. Wetteraeur, A. Pusel, and P. Hess, *Chem. Phys. Lett.* **300**, 397 (1999).
- [12] K. Sinniah, M. G. Sherman, L. B. Lewis, W. H. Weinberg, J. T. Yates, Jr., and K. C. Janda, *Phys. Rev. Lett.* **62**, 567 (1989).
- [13] M. L. Wise, B. G. Koehler, P. Gupta, P. A. Coon, and S. M. George, *Surf. Sci.* **258**, 166 (1991).
- [14] J. W. Sharp and G. Eres, *Surf. Sci.* **320**, 169 (1994).
- [15] T. Ligget, *Interacting Particle Systems* (Springer-Verlag, New York, 1985).
- [16] N. G. Van Kampen, *Stochastic Processes in Physics and Chemistry* (North-Holland, Amsterdam, 1981).
- [17] R. Brown and N. A. Efremov, *Chem. Phys.* **155**, 357 (1991).
- [18] S. F. Burlatsky and G. Oshanin, *J. Stat. Phys.* **65**, 1095 (1991).
- [19] D. C. Torney and H. M. McConnell, *J. Phys. Chem.* **87**, 1941 (1983).
- [20] J. L. Spouge, *Phys. Rev. Lett.* **60**, 871 (1988).
- [21] P. Argyrakis and R. Kopelman, *Phys. Rev. A* **41**, 2114 (1990).
- [22] A. Lin, R. Kopelman, and P. Argyrakis, *Phys. Rev. E* **53**, 1502 (1996).
- [23] P. Argyrakis and R. Kopelman, *Chem. Phys.* **261**, 391 (2000).
- [24] B. Ben-Avraham and S. Havlin, *Diffusion and Reactions in Fractals and Disordered Systems* (Cambridge University Press, Cambridge, England, 2000).
- [25] T. O. Masser and D. ben-Avraham, *Phys. Rev. E* **64**, 062101 (2001).
- [26] E. Clément, L. M. Sander, and R. Kopelman, *Phys. Rev. A* **39**, 6472 (1989).
- [27] W.-S. Sheu, K. Lindenberg, and R. Kopelman, *Phys. Rev. A* **42**, 2279 (1990).
- [28] S. Habib, K. Lindenberg, G. Lythe, and C. Molina-París, *J. Chem. Phys.* **115**, 73 (2001).
- [29] L. W. Anacker and R. Kopelman, *J. Chem. Phys.* **81**, 6402 (1984); L. W. Anacker, R. P. Parson, and R. Kopelman, *J. Phys. Chem.* **89**, 4758 (1985); L. W. Anacker, R. Kopelman, and J. S. Newhouse, *J. Stat. Phys.* **36**, 591 (1984).
- [30] C. Nassif and P. R. Silva, *Mod. Phys. Lett. B* **15**, 1205 (2001).
- [31] Z. Rácz, *Phys. Rev. Lett.* **55**, 1707 (1985).
- [32] J.-M. Park and M. W. Deem, *Eur. Phys. J. B* **10**, 35 (1999).
- [33] S. F. Burlatsky and A. I. Chernoutsan, *Phys. Lett. A* **145**, 56 (1990).
- [34] B. Bonnier, *Phys. Rev. E* **58**, 5424 (1998); B. Bonnier and R. Brown, *ibid.* **55**, 6661 (1997); B. Bonnier, R. Brown, and E. Pommiers, *J. Phys. A* **28**, 5165 (1995).
- [35] V. M. Kenkre and H. M. Van Horn, *Phys. Rev. A* **23**, 3200 (1981).
- [36] S. N. Majumdar and V. Privman, *J. Phys. A* **26**, L743 (1993).
- [37] F. Baras, F. Vikas, and G. Nicolis, *Phys. Rev. E* **60**, 3797 (1999).
- [38] E. Abad, P. Grosfils, and G. Nicolis, *Phys. Rev. E* **63**, 041102 (2001).

- [39] F. Vikas, F. Baras, and G. Nicolis, *Phys. Rev. E* **66**, 036133 (2002).
- [40] G. Oshanin, S. F. Burlatsky, E. Clément, D. Graff, and L. M. Sander, *J. Phys. Chem.* **98**, 7390 (1994).
- [41] M. Hoyuelos, *Phys. Rev. E* **50**, 2597 (1994).
- [42] J. W. Lee, *J. Chem. Phys.* **117**, 7864 (2002).
- [43] W. J. Chung and M. W. Deem, *Physica A* **265**, 486 (1999).
- [44] A. L. Parrondo and H. O. Martín, *Physica A* **273**, 360 (1999).
- [45] G. Oshanin and S. F. Burlatsky, *Phys. Rev. E* **67**, 016115 (2003).
- [46] P. Argyrakis, S. F. Burlatsky, E. Clement, and G. Oshanin, *Phys. Rev. E* **63**, 021110 (2001).
- [47] L. K. Gallos and P. Argyrakis, *Phys. Rev. Lett.* **92**, 138301 (2004).
- [48] L. Braunstein, H. O. Martín, M. Grynberg, and H. E. Roman, *J. Phys. A* **25**, L255 (1992).
- [49] M. Hoyuelos and H. O. Martín, *Phys. Rev. E* **48**, 3309 (1993).
- [50] V. Privman, C. R. Doering, and H. L. Frisch, *Phys. Rev. E* **48**, 846 (1993).
- [51] H. O. Martín, J. L. Iguain, and M. Hoyuelos, *J. Phys. A* **28**, 5227 (1995).
- [52] M. Bowker, *The Basis and Applications of Heterogeneous Catalysis* (Oxford University Press, Oxford, 1998).
- [53] V. P. Zhdanov, *Elementary Physicochemical Processes on Surfaces* (Plenum, New York, 1991).
- [54] P. Córdoba-Torres, R. P. Nogueira, and V. Fairén, *J. Electroanal. Chem.* **560**, 25 (2003).
- [55] M. Malek Mansour and J. Houard, *Phys. Lett.* **70A**, 366 (1979).
- [56] N. G. Van Kampen, *Stochastic Methods in Physics and Chemistry* (North-Holland, Amsterdam, 1981).
- [57] S. Prakash and G. Nicolis, *J. Stat. Phys.* **82**, 297 (1996).